Iron doping in the deoxygenated $YBa_2(Cu_{1-x}Fe_x)_3O_y$ compounds

I. Mirebeau
Laboratoire Léon Brillouin, Centre d'Etudes Nucléaires de Saclay, 91191 Gif-sur-Yvette Cedex, France

E. Suard and V. Caignaert
Laboratoire CRISMAT, Institut des Sciences de la Matière et du Rayonnement, Université de Caen, 14050 Caen, France

F. Bourée
Laboratoire Léon Brillouin, Centre d'Etudes Nucléaires de Saclay, 91191 Gif-sur-Yvette Cedex, France
(Received 28 January 1994)

Neutron powder-diffraction measurements have been performed to determine the magnetic phase diagram of the $YBa_2(Cu_{1-x}Fe_x)_3O_y$ system for an oxygen concentration y close to 6.2. The temperature and concentration dependence of the magnetic moments on the Cu_1 and Cu_2 sites have been deduced from Rietveld refinements. At low temperature, the results show the occurrence of a noncollinear phase for $x < 0.03$. At higher iron content, a collinear phase is observed, with a doubling of the magnetic unit cell along the c axis, and a moment μCu_1 on the Cu_1 sites whose absolute value increases with iron content. The succession of magnetic phases is well understood by a simple energy calculation. In the collinear phase, the sign of μCu_1 with respect to the moment on the neighboring Cu_2 sites is correlated to the local iron environment and can be modified through an appropriate heat treatment.

INTRODUCTION

Iron substitution in the oxygenated ($y = 7$) compounds of the 123 family results in a rather slow decrease of the superconducting temperature, since a zero T_c value is obtained for the maximum possible doping content $x = 0.15$ (Ref. 1). This small effect contrasts with that of the Zn substitution, where a small doping of about 4% with the nonmagnetic Zn considerably reduces the superconducting region.[2] This peculiarity of the Fe substitution is generally explained by considering that the trivalent iron ions mainly substitute to the charge reservoirs Cu_1 and not to the superconducting planes Cu_2, so that the decrease of T_c comes from charge-transfer effects and not from magnetic pair breaking. In the deoxygenated compounds, several magnetic phases have been observed depending on oxygen concentration. This is shown in the $YBa_2Cu_3O_y$ system,[3,4] but also in related systems like $NdBa_2Cu_3O_y$ (Refs. 5 and 6), or $YBa_2(Cu_{1-x}Co_x)_3O_y$ (Ref. 7). The succession of these phases has also been related to charge-transfer effects, the noncollinear phases being observed for low charge transfers and collinear one for higher ones. The physical reason invoked for this phenomenon is that the hole doping in the chain sites creates Cu^{2+} ion with spins and frustrates the antiferromagnetic (AF) coupling between next-nearest-neighbors Cu_2 layers. These experimental results have been supported by Monte Carlo simulations in a random (quenched) state of the doping holes.[8] However, the precise nature of the antiferromagnetic, or superconducting, state could also depend on the local order of the doping holes in the charge reservoirs. This has been shown in the $YBa_2Cu_3O_y$ system, where the superconducting temperature, for a given oxygen content, depends on the sample heat treatment, and where the ordering of the oxygen chains determine the superconducting plateau around 60 K.[9] In the antiferromagnetic side of the phase diagram, a similar effect has been observed in the Co-substituted 123 compound, where the nature of the AF phase depends on the local order of the $3d$ ion.[10]

In the $YBa_2(Cu_{1-x}Fe_x)_3O_y$ system, an increase of iron doping yields a change in the charge balance similar to a decrease in the oxygen content. One interest of the iron doping is that the local environment of iron, and its substitution rate on the Cu_1 and Cu_2 sites can be related to the observed magnetic order, by comparing Mössbauer or nuclear quadrupole resonance measurements to neutron results.[11,12]

At high Fe and oxygen content, a collinear antiferromagnetic phase was previously observed, which consisted of alternating AF planes along the c axis.[12,13] We present here a systematic study of iron doping in the concentration range $0 < x < 0.08$ for a given oxygen content y close to 6.2. We have observed for low iron content ($x < 0.03$), the competition between two collinear antiferromagnetic phases, resulting in a noncollinear phase at low temperature. In this concentration range, the mean moment on the Cu_1 sites remains very small. At higher iron content, a collinear phase persists alone, with a spin value in the Cu_1 and Cu_2 sites increasing with iron concentration. In this concentration range, frustration effects due to the freezing of paramagnetic Fe spins are observed. In a brief report on these data,[14] the antiferromagnetic phase diagram was determined by performing Gaussian fits of the magnetic peaks. We now present a more complete analysis, performed through Rietveld refinements of the spectra. We discuss the stability of the magnetic phases in comparison with the results in undoped and Co-doped compounds when oxygen concentration is varied. We also show that the stability of these phases strongly de-

0163-1829/94/50(5)/3230(9)/$06.00

pends on the local iron environment and can be modified through an appropriate heat treatment.

I. SAMPLE PREPARATION AND HEAT TREATMENT

We have studied polycrystalline samples of iron and oxygen concentrations $x=0.01$ ($y=6.21$), 0.02 ($x=6.10$ and 6.15), 0.03 ($y=6.20$), 0.06 ($y=6.22$), and 0.08 ($y=6.24$). They were prepared in the usual manner, following the procedure described in (Ref. 11), and were deoxygenated at high temperature ($T=850\,^{\circ}\mathrm{C}$), by heating the samples under an argon atmosphere during 24 h. Another sample with $x=0.06$ and $y=6.15$ was deoxygenated at a much lower temperature (350 °C) in presence of zirconium. This second deoxygenation process yields an iron occupation on the Cu_1 and Cu_2 sites closer to the thermodynamical equilibrium at room temperature whereas the usual process corresponds to a quenching of the occupation rates from a high-temperature state. The oxygen content was determined by thermogravimetric analysis and neutron refinements of the nuclear structure, the error bar on y being equal to ± 0.05.

During the sample preparation or deoxygenation process some impurity phases could be formed. We have systematically rejected the samples where some impurity peaks could be observed on x-ray data. In the samples studied here, the intensity of these peaks is generally 1000 times smaller and never exceeds $\frac{1}{100}$ of the intensity of the main Bragg reflections.

II. NEUTRON-DIFFRACTION EXPERIMENTS

Diffraction experiments have been performed in the temperature range $8<T<460$ K, on the spectrometer G6-1 of the reactor Orphée at Laboratoire Léon Brillouin (LLB), using a multidetector of 400 cells and a long neutron wavelength on 4.73 Å. These conditions permitted us to obtain a good statistical precision and resolution on the magnetic peaks, whose intensity was comparable to that of impurity peaks. However, the scattering vector range was limited to $0.1<q<2.5$ Å^{-1}. Consequently, for some samples we have also measured a diffraction spectrum at room temperature on the high-resolution spectrometer 3 T2 at LLB with a much shorter wavelength of 1.227 Å. This allowed us to get a better determination of the nuclear parameters (atomic positions in the unit cell, oxygen concentration, Debye-Waller factors).

We have analyzed the experimental data in two ways. In a first step, we have determined the temperature dependence of the magnetic Bragg peaks by fitting them separately using a Gaussian shape. This allowed us to determine the transition temperatures, but also to evidence small anomalies of the peak widths or intensities.[14] In a second step, as described below, we have analyzed the magnetic structure in its whole through Rietveld refinement of the spectra. We could thus determine the temperature and concentration dependence on the mean magnetic moments on the Cu_1 and Cu_2 sites separately. In these refinements, the nuclear agreement factors R_N were very good (around 3%), but the magnetic factors R_M were much worse (between 5% and 15% at low temperature) and rather sensitive to the definition of the background and to the presence of impurities.

Consequently, the background was carefully determined at each temperature. As for the impurities, since we could not identify them, we could not include them as a second phase in the Rietveld refinement. We have studied their influence by the following method. Spectra above the Néel temperature were measured to check the "nuclear" nature of these peaks. When they overlap some of the magnetic peaks, as shown for instance in Fig. 1(a), the spectra of the impurities above T_N were subtracted from the data below T_N. This could only be done above room temperature, since the experimental conditions are slightly different below. The main result of the subtraction is to decrease the uncertainty on the mo-

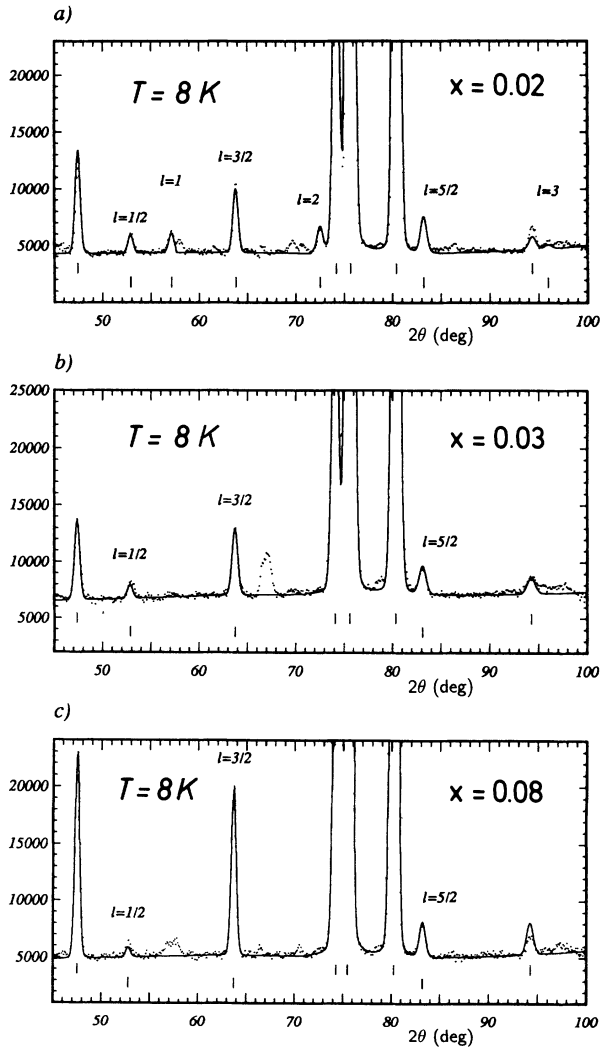

FIG. 1. Rietveld refinements of the neutron spectra in the $YBa_2(Cu_{1-x}Fe_x)_3O_y$ system (y close to 6.2), focusing on the magnetic Bragg peaks. (a) $x=0.02$, (b) $x=0.03$, (c) $x=0.08$. In (b) the peak at 67° comes from the cryogenerator background. It could be suppressed for most of the other samples. The other peaks come from impurities, as discussed in the text.

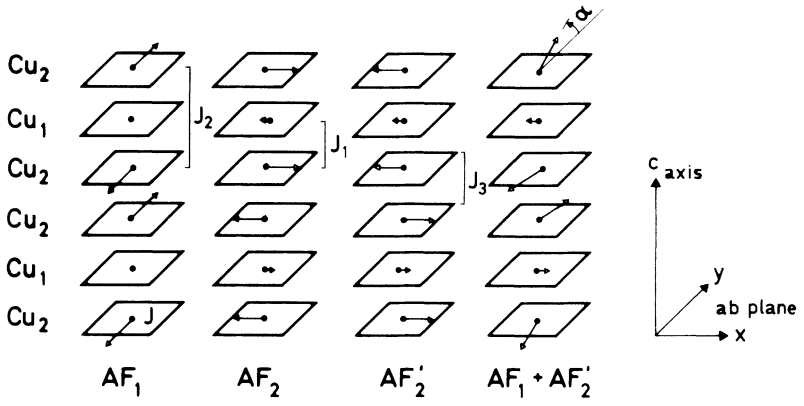

FIG. 2. Schematic description of the magnetic structures AF_1, AF_2, AF_2', and of the mixed phase AF_1+AF_2', as described in the text. We have indicated the coupling constants J_1, J_2, J_3, and the tilting angle α.

ments values and the magnetic R factors, but the moments themselves remain unchanged.

A. The low-concentration range ($x < 0.03$)

At low iron content ($x = 0.01, 0.02$), the spectra measured at the lowest temperature of 8 K [Fig. 1(a)], clearly show the coexistence of two types of magnetic reflections ($\frac{1}{2}\ \frac{1}{2}\ l$) with integer l and half-integer l values respectively. With increasing temperature, the intensity of the half-integer l reflections decreases at the benefit of the integer l ones. This behavior, similar to that observed in the undoped compound with $y = 6.35$ (Refs. 3 and 4), can be described by a competition between two collinear structures, which coexist at low temperature, leading to a noncollinear phase.

The structure with integer l reflections AF_1, corresponds to the structure of the undoped compound with $y = 6$ (Ref. 3). It is described by a stacking sequence $+0-+0-$ of antiferromagnetic planes along the c axis, without any moment in the Cu1 sites (Fig. 2). It involves an AF coupling between next-near-neighbors Cu_2 planes.

In the second structure, the existence of half-integer l reflections is related to the presence of an ordered spin in the Cu_1 sites, which doubles the unit cell along the c axis. This structure can be equivalently described by $a+-+-+-$ stacking of AF planes (AF_2-type), or by a $++--+-$ stacking (AF_2'-type). These two variants of the same structure only differ by the sign of the coupling between near neighbors Cu_1-Cu_2 planes. In the convention chosen here, AF_2 (resp. AF_2') corresponds to antiparrallel (resp. parallel) spin components of Cu_1-Cu_2 near neighbors. A calculation of the intensities of the half-integer l peaks is shown in Fig. 3 as a function of the ratio r between the spins components in the Cu_1 and Cu_2 sites. In the AF_2 type ($r < 0$), we see that the intensity of the $l = \frac{3}{2}$ peak is much stronger than the intensities of the $l = \frac{1}{2}$ and $\frac{5}{2}$ ones, whereas in the AF_2' type ($r > 0$), the intensities of these three peaks are of comparable magnitude.

Magnetic Rietveld refinements were performed by assuming a linear superposition of the AF_1 and AF_2 (or AF_2') structures with spin components lying, respectively, along two orthogonal axes x and y in the ab plane. These refinements were made using the program FULLPROF.[15] The component μCu_2^y is relative to the AF_1 structure, whereas the components μCu_2^x and μCu_1^x refer to the AF_2 (or AF_2') structure. The angle between the x and y directions with respect to the a and b axis of the nuclear cell could not be determined due to the tetragonal nature of the unit cell. Other Rietveld refinements performed by assuming spin components parallel to the c axis yield a much worse agreement with the experimental data.

The temperature dependence of the magnetic moments is shown in Fig. 4(a) for the $x = 0.01$ sample. At high temperature ($T < T_{N1}$ where $T_{N1} = 420 +/- 10$ K), the AF_1 phase exists alone. Below a temperature T^* of about

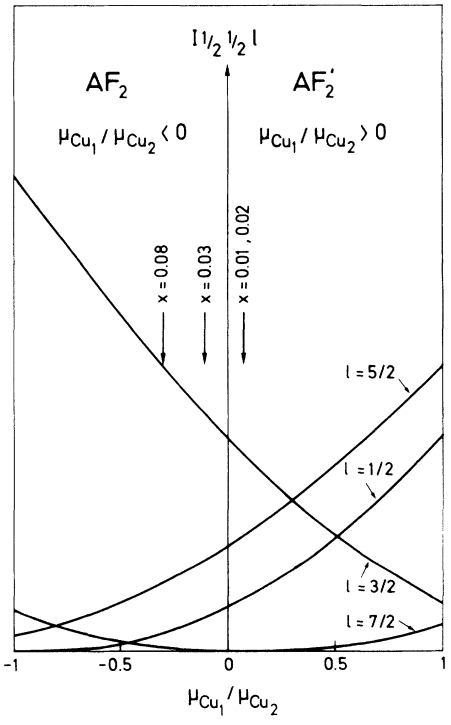

FIG. 3. Calculation of the intensities of the $\frac{1}{2}\ \frac{1}{2}\ l$ Bragg peaks ($l = \frac{1}{2}, \frac{3}{2}, \frac{5}{2}, \frac{7}{2}$) as a function of the ratio $\mu Cu_1/\mu Cu_2$ in the collinear phase. A negative (resp. positive) value of this ratio corresponds to the AF_2 (resp. AF_2') structure. We have assumed spin components perpendicular to the c axis.

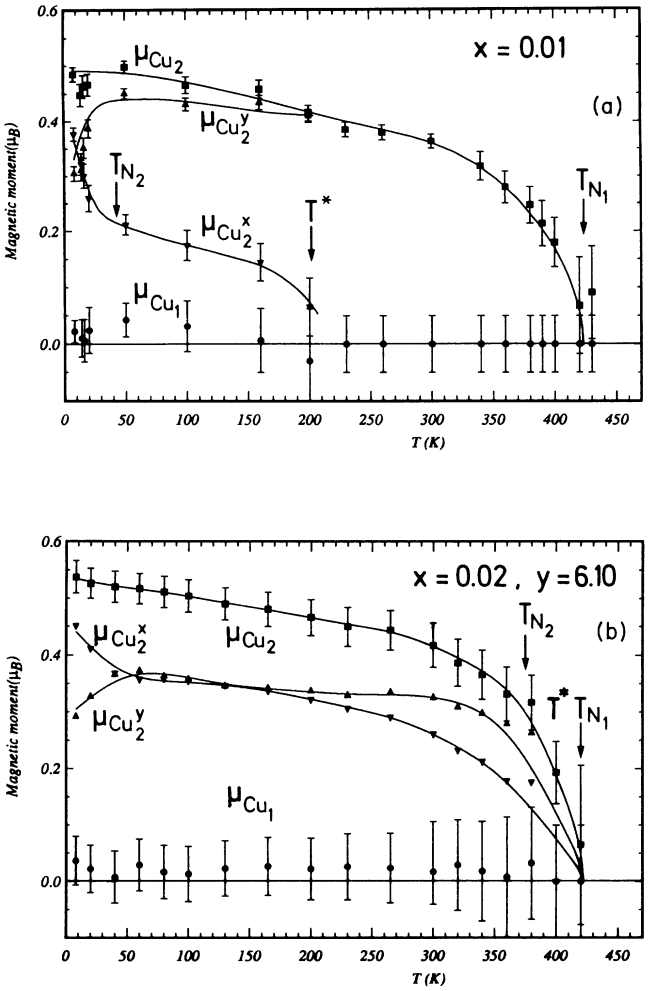

FIG. 4. Temperature dependence of the mean ordered moments. (a) For $x=0.01, y=6.21$; (b) for $x=0.02, y=6.10$.

200 K, a small moment appears in the Cu_1 sites, as shown by the occurrence of very small and broad half-integer l reflections. In the range $T_{N2}<T<T^*$, Gaussian fits of these magnetic peaks show that their width remains slightly larger than that of the spectrometer resolution, showing that a long-range order of the AF_2' phase is not completely achieved. Below T_{N2}, where T_{N2} is around 40 ± 10 K, the half-integer l peaks become thinner and their intensity suddenly increases. This corresponds to an increase of the spin component μCu_2^x. Concomitantly, there is a decrease of the component μCu_2^y. The total spin the Cu_2 layers, μCu_2 shows no anomaly with temperature. Clearly the occurrence of moments in the Cu_1 layers, tilts the moments in the Cu_2 ones, with a much stronger effect when the Cu_1 spins become long-ranged ordered.

Similar results are observed for the sample with $x=0.02, y=6.15$. The $l=\frac{1}{2}$ peaks become broad and almost nonvisible above $T_{N2}=110$ K, but short-ranged correlations of the same nature persist up to a T^* value of about 150–200 K, the Néel temperature of the AF_1 phase being equal to about 410 K (± 10 K). Clearly, for these two samples, there is a progressive building of the AF_2-AF_2' phase, resulting in a noncollinear long-ranged ordered structure in the low-temperature range. In the second $x=0.02$ sample with $y=6.10$ [Fig. 4(b)], the noncollinear structure persists up to $T_{N2}\approx 370$ K, and the short-range correlations are observed close to the Néel temperature of the AF_1 phase ($T^*\approx T_{N1}=415$ K ± 10 K). As in the two other samples, we observe around 100 K a sudden increase of the tilting angle α, as defined by $tg\alpha=\mu Cu_2^x/\mu Cu_2^y$ (Fig. 5). In all these samples, the mean spin on the Cu_1 sites remains very small, of about 0.02 μB/atom. Consequently, its sign cannot be ascertained, but the overall results suggest an AF_2' structure ($r\geq 0$). The temperature dependence of the total spin on the Cu_2 sites, can be fitted with a law $\mu Cu_2 \propto (T-T_N)^\beta$, yielding a critical exponent β close to 0.2.

B. The high-concentration range ($x \geq 0.03$)

Above $x=0.02$, the Bragg peaks with integer l values are no more visible and the magnetic intensities can be refined assuming a collinear structure. In this concentration range, the mean spin value on the Cu_1 sites is sufficiently high so that the sign of the Cu_1-Cu_2 coupling can be determined unambiguously. We find an antiparallel arrangement between Cu_1 and Cu_2 layers (AF_2 type). As x increases [Fig. 1(b) and 1(c)], the growing of the $l=\frac{3}{2}$ peak at the expense of the other magnetic ones reflects the increase of μCu_1 with iron concentration. It becomes of the same order of magnitude as μCu_2 at high x values.

In this concentration range, the temperature dependence of the magnetic moments (Fig. 6), shows some small anomalies. For $x=0.03$, a small minimum in the variation of μCu_2 around 50 K seems to be related to a decrease in the coherence length of the ordered structure, since Gaussian fits of the magnetic intensities show a slight enlargement of the peak width. Above $x=0.03$, we observe a slight but systematic decrease of the ordered spins on Cu_1 and Cu_2 sites in the low-temperature range. This effect was studied in more detail in a $x=0.12, y=6.5$ sample, by comparing neutron-diffraction results to Mössbauer and inelastic neutron

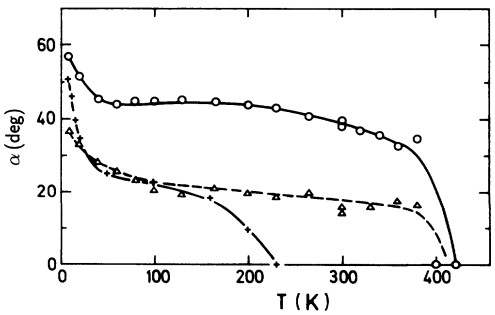

FIG. 5. Temperature dependence of the tilting angle α in degree for $x=0.01$, (+), $x=0.02$, ($y=6.15$), (△) and $x=0.02$ ($y=6.10$) (○).

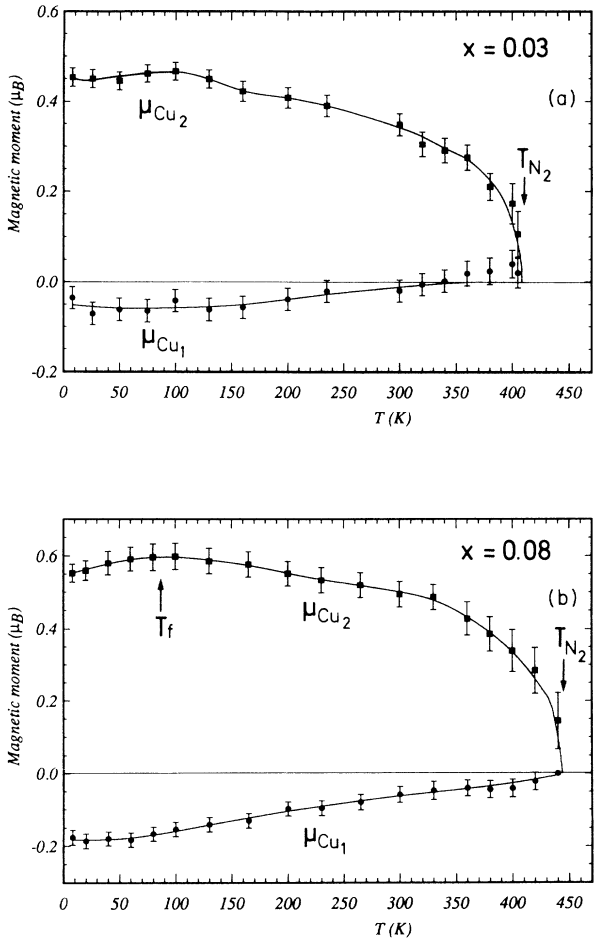

FIG. 6. Temperature dependence of the mean ordered moments in μB/atom. (a) For $x=0.03$, (b) for $x=0.08$. The freezing temperature T_f is indicated by an arrow.

scattering.[11] It can be attributed to the freezing of frustrated paramagnetic iron spins in the Cu_1 sites. In the chain sites, the frozen iron spins seem to follow the principal axis of the electric-field gradient, which can vary locally with the oxygen environment. The freezing of iron spins below T_f induces a canting of the neighboring Cu_1 spins, and a decrease of the ordered component μCu_1, mostly due to in-plane disorder. In the Cu_2 plane, much less disorder should be expected, since the oxygen environment is always the same, and the hyperfine field of the Fe atoms in the Cu_2 sites shows no anomaly with temperature. The decrease of the long-ranged ordered component μCu_2 is therefore attributed to out-of-plane disorder, coming from stacking faults in the periodicity along the c axis.

III. DISCUSSION

The phase diagram of the system is plotted in Fig. 7, where we have reported the concentration dependence of the Néel temperatures T_{N1} and T_{N2}, and of the freezing temperature T_f. For $x<0.03$, short-range antiferromagnetic correlations of the AF_2 type are observed below T^*,

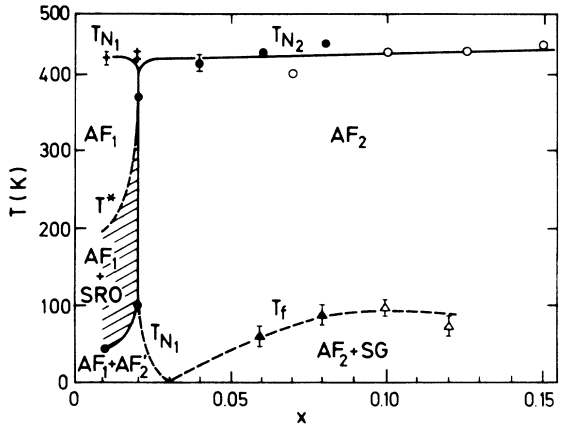

FIG. 7. Magnetic phase diagram of the $YBa_2(Cu_{1-x}Fe_x)_3O_y$ ($y\approx 6.2$) system: concentration dependence of the Néel temperatures T_{N1} and T_{N2} and of the freezing temperature T_f. The onset of short-ranged correlations below T^* are indicated by dashed lines. The values for $x=0.07$, 0.10, 0.15 ($y\approx 6.4$) are from Ref. 16.

with $T_{N2}\leq T^*\leq T_{N1}$, as shown by dashed areas in the figure. With increasing x, T_{N2} increases and reaches T_{N1} for $x=0.02$. Between 0.02 and 0.03, we observe a steplike change in the magnetic order, as T_{N1} abruptly decreases from 400 K to zero. Then above $x=0.03$, T_{N2} slowly increases with increasing x. The freezing temperature T_f also increases with iron doping.

In Fig. 8, we have plotted the concentration dependence of the mean magnetic moments, determined at low temperature (8 K). In the low-concentration range, we observe an increase of μCu_2^x with increasing x, together with a decrease of μCu_2^y, but the total magnetic moment μCu_2 does not strongly depend on x and remains close to its values in the $YBa_2Cu_3O_{6.2}$ compound (0.6 μB/atom as determined in Ref. 4). In the collinear phase, the moments on both sites increase with iron substitution, but the main effect arises as expected on the Cu_1 sites. We have also added on Figs. 7 and 8, the values obtained for

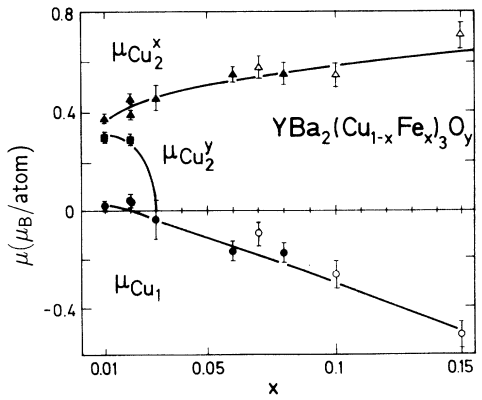

FIG. 8. Concentration dependence of the magnetic moments on the Cu_1 and Cu_2 sites as measured at 8 K. The values for $x=0.07$, 0.10, 0.15 are from Ref. 16.

three isotopically enriched samples with higher oxygen and iron contents ($x=0.07$, 0.10, and 0.15, $y\approx 6.4$ from Ref. 16), which appear to be in good agreement with our data. At high iron content, the magnetic effect of iron is so strong that a slight increase in the oxygen content should not change much the spin values and Néel temperatures.

The magnetic phase diagram shows striking similarities with the one of the Co-doped compound, when oxygen concentration is varied from 6.2 to 6.8 at fixed Co content ($x=0.07$, see Ref. 6). In both cases, we observe that the noncollinear phases are seen at low charge transfer (low iron doping or high oxygen content which accommodates the excess Co^{3+} charge). A similar situation is encountered in $NdBa_2Cu_3O_y$ system.[5,6]

In the nonsubstituted $YBa_2Cu_3O_{6.2}$, the distribution of Cu valence states in the chain sites can be evaluated to about $\frac{1}{3}$ of Cu^+ ions and $\frac{2}{3}$ of Cu^{2+} ions.[17,18] The substitution of Fe^{3+} in the chain sites should decrease the number of holes in the neighboring coppers ($Cu^{2+}\rightarrow Cu^+$) or change the valency of the neighboring oxygens ($O^-\rightarrow O^{2-}$), in order to accommodate the excess of positive charge. The precise nature of this charge transfer within the chains depends on the length of the chains. Only rather long chains with three or more oxygens can accommodate the Fe^{3+} ions without decreasing the number of Cu^{2+} spins. In any case, the possible suppression of Cu^{2+} spins in the chains is overcome by the strong magnetic moment brought by the Fe^{3+} spins (about 5 μB/atom Fe), so that iron substitution will bring a net magnetic moment in the substituted Cu_1 sites. The existence of μCu_1 frustrates the antiferromagnetic coupling (J_2) between next neighbors Cu_2 layers, leading to the observed changes ($AF_1\rightarrow AF_1+AF_2\rightarrow AF_2$) in the magnetic phases. The first transition to the mixed phase is also seen in the nonsubstituted compound at higher oxygen content ($y=6.35$, see Refs. 3 and 4), due to the magnetic moments localized on the Cu atoms of the short oxygen chains.

A. Nature and stability of the mixed AF_1+AF_2 phase

In the study of the phase stability, a question arises about the nature—homogeneous or inhomogeneous—of the mixed phase AF_1+AF_2. Namely, do we observe a real noncollinearity within the unit cell, or a coexistence of large domains of the two distinct collinear phases? The first hypothesis is supported, as is noted in Ref. 4, by the fact that no hysteresis is observed in the temperature dependence of the magnetic Bragg peaks. Within this hypothesis, the energy of the mixed phase is written, according to Ref. 4 as a function of the interplane exchange integrals J_i, the tilting angle α, and the amplitude σ of the ratio between the spins on both sites ($\sigma=|\mu Cu_1/\mu Cu_2|$). Assuming a negligible planar anisotropy, the energy is written, within the molecular-field approximation:

$$E=J_3-2J_1\sigma\sin\alpha+J_2\cos(2\alpha)$$

or equivalently,

$$E=J_3+J_2-2J_1\sigma\sin\alpha-2J_2\sin^2\alpha\ .$$

In this expression, we have chosen the standard convention, by contrast with Ref. 4, so that a positive J value corresponds to a ferromagnetic coupling. J_1 is the exchange integral coupling the Cu_1 layers and the Cu_2 ones: $J_1<0$ (resp. >0) corresponds to the AF_2 (resp. AF_2') structure. J_2 is the coupling between next-nearest neighbors Cu_2 layers ($J_2<0$). J_3 is the coupling between near neighbors Cu2 layers ($J_3<0$). The frustration arises from the antiferromagnetic character of J_2. According to inelastic measurements in the $YBa_2Cu_3O_6$ compound,[17] J_2 and J_3 are related to the exchange integral J within the Cu_2 plane ($|J|=0.17$ eV) through the relations $J_2/J\approx 3.5\times 10^{-5}$ and $J_3/J\approx 8.5\times 10^{-2}$.

The energy is plotted as a function of the tilting angle α in Fig. 9(a), for several values of the ratio σ, assuming a positive J_1 value. For $\sigma=0$, the energy is minimized for $\alpha=0$, which corresponds to the AF_1 phase. In the intermediate range $0<\sigma<|2J_2/J_1|$, the noncollinear phase is stabilized with a tilting angle α_0 ($\sin\alpha_0=-J_1\sigma/2J_2$). As σ increases, the α_0 value tends to the value obtained for the collinear AF_2' phase ($\alpha=\pi/2$). For σ values greater than $|2J_2/J_1|$, the AF_2' phase minimizes the energy. We note that the instability of the mixed phase should be observed whatever the sign of J_1, a negative J_1 value stabilizing the AF2 variant ($\alpha=-\pi/2$). The energy diagram showing the respective stabilities of all phases is shown in Fig. 9(b). Such an evolution of the phases stability can be considered either as a function of temperature or when varying the iron concentration, if we neglect the entropic term. From the value of σ and of the tilting angle α at low temperature in the $x=0.01$ and 0.02 samples, we deduce a ratio $|J_1/J_2|$ of about 30–40. We can use this result to get an order of magnitude for the value of μCu_1, where the mixed phase should become unstable. We expect that it should disappear for $\mu Cu_1>0.03$ μB/atom, in good agreement with the experimental observations for the $x=0.03$ sample. Experimentally, the transition to the collinear phase seems to be associated with a change in the sign of the J_1 coupling. This could be related to some changes in the local order of iron as discussed below.

The effect of spin frustration in the $YBa_2Cu_3O_y$ system has also been considered through Monte Carlo simulations.[8] In this "quenched" model the authors consider a random distribution of holes either in the Cu_1 or in the Cu_2 layers. A hole added to a Cu^+ ion in the chain sites creates a Cu^{2+} ion with a spin, whereas a hole entering in the Cu_2 layers should sit in an oxygen site and eliminate a neighboring Cu^{2+} spin through the formation of a singlet state. Consequently, hole doping in the Cu_2 planes only results in a decrease of the Néel temperature of the AF_1 phase by spin dilution, whereas hole doping in the Cu1 planes induces a magnetic transition towards an AF_2 like phase. As discussed above, this second situation is close to that encountered by iron substitution at low iron content. Interestingly enough the Monte Carlo simulations show that the phase boundary between the AF_1 and AF_2 (or AF'2) phases favors AF_1 at high temperature, since

the totally frustrated spins in the AF_1 phase generate larger entropy than in the AF_2 one. This argument led the authors to conclude that the transition between the two phases was of first order, and occurred for a value of the ratio σ close to J_2/J_1 at $T=0$, with an inhomogeneous coexistence of the two phases near the phase boundary. We recall that it is only valid for a random spin distribution in the Cu_1 layers.

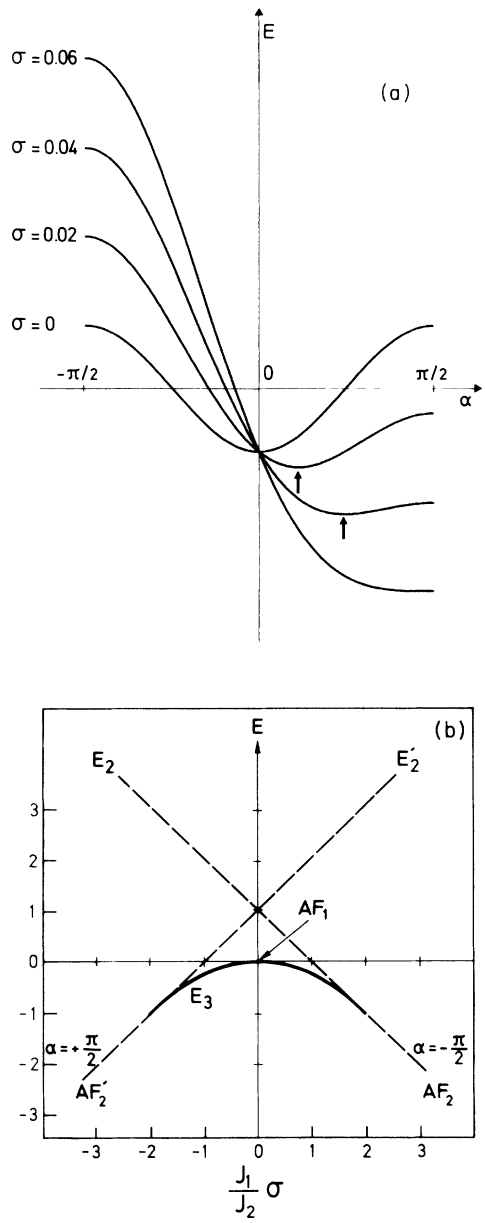

FIG. 9. Energy E in arbitrary units as a function of the tilting angle α, for several values of the ratio between the spins on both sites ($\sigma=|\mu Cu_1/\mu Cu_2|$). The zero energy value corresponds to J_3; the coupling constants J_1 and J_2 verify $J_1/J_2=-35$; (a) $\sigma=0$ (stabilization of the AF1 phase, for $\alpha_0=0$); (b) $\sigma=0.02$ (stabilization of the mixed phase with tilting angle $\alpha_0=20°$); (c) $\sigma=0.04$ ($\alpha_0=44°$); (d) $\sigma=0.06$ (stabilization of the AF_2 phase with $\alpha_0=90°$). (b) Energy diagram showing the stability of the different phases with respect to the parameter $J_1\sigma/J_2$; E_2, E'_2, and E_3 are, respectively, the energies of the phases AF2, AF'2 and of the mixed phase.

B. Mutual stability of the AF_2 and AF'_2 structures

The mutual stability of these two variants of the same structure, which only differ by the sign of the J_1 coupling has been already discussed.[5] In principle, the AF'_2 structure should be favored, considering the symmetry of the orbitals involved in the Cu_1 and Cu_2 layers. In the Cu_2 sites, due to the square oxygen environment, the holes belong to orbitals of the symmetry $3d$ (x^2-y^2). In the chain sites, assuming small chains in the y axis for instance, the holes would belong to the orbitals $3d$ (z^2-y^2), which can hybridize with the $3d$ $(3z^2-r^2)$ orbital of the neighboring Cu_2 site. Consequently, according to the Hund's rule, a ferromagnetic coupling between the Cu_1 and Cu_2 spins should be expected. This argument was used to justify the stability of the $NdBa_2Cu_3O_y$ magnetic phase[5] as well as the ferromagnetic coupling in K_2CuF_4 (Ref. 19). However, we must also take into account the local changes induced in the hole environments by the Fe (or Co) substitution.

In the Cu_2 layers, the few substituted Fe likely change the oxygen environment, in order to decrease the Coulomb repulsion. This could be achieved either by attracting excess oxygens below the layer in order to build an octahedral environment, or by moving towards the center of the pyramid. Both reasons could explain the small quadrupolar gradient measured on these sites in Mössbauer experiments.[20] In the Cu_1 layers the chain configuration can also be changed with iron substitution. For instance, in the undoped compound with $y=6.2$, the chains in the Cu_1 layers involve only one or two oxygens, disposed in a tetragonal arrangement. This is shown by neutron diffraction[21] and justified by energy calculations.[17] Without iron, longer chains with three oxygens only form at higher oxygen content ($y=6.4$), when superconductivity starts.[17,22] It is likely that such longer chains with three or more oxygens could also form for $y=6.2$ around the iron ions of the substituted compound. The oxygen environment of the magnetic atoms (Fe^{3+} or Cu^{2+}) could influence the type of magnetic order in two ways: (i) the length of a given oxygen chain will govern the number of Cu^{2+} spins within it, considering the internal charge transfers. (ii) The symmetry of the orbitals where the holes are situated can be directly affected (superexchange or cooperative Jahn-Teller effect).

We have now started to study the AF order as a function of the heat treatment, in the collinear phase. We have investigated two samples with the same iron and oxygen concentration ($x=0.06, y=6.2$). The sample (a) has received the usual deoxygenation process at high temperature described above. The sample (b) has been deoxygenated at a lower temperature. The results show that we can switch the stability of the AF_2 structure by controlling the local order of Fe and its repartition within the Cu_1 and Cu_2 layers. Figure 10 shows the temperature dependence of the means moments of both samples. The Néel temperatures are almost the same, but that in sam-

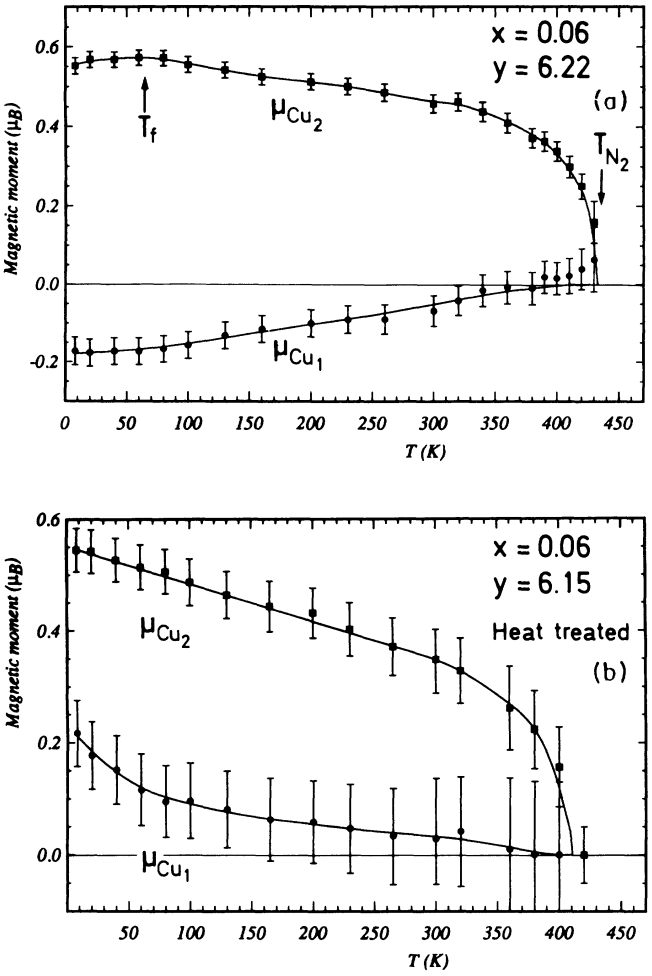

FIG. 10. Influence of the heat treatment on the mean ordered moments for the concentration $x=0.06$, $y\approx 6.2$. (a) High-temperature deoxygenation. (b) Low-temperature deoxygenation (see text).

ple (b) we now observe ferromagnetic coupling between Cu_1 and Cu_2 layers instead of the antiferromagnetic one. Moreover, the freezing of iron spins at low temperature (around 30 and 60 K, respectively) does not have the same effect in the two samples. In sample (a) it frustrates the long-range order on the copper lattice (decrease of μCu_2), whereas in sample (b) it enhances this order (increase of the ordered spin μCu_1).

We are now performing Mössbauer measurements in these two samples, in order to relate the observed changes to the iron local environments and occupancies. The first results suggest that in sample (a), 35% of the iron atoms have moved to the Cu_2 sites, the remaining Fe being gathered in rather long chains, in order to share a pyramidal oxygen environment. By contrast, in sample (b), only 14% of the iron atoms are situated in the Cu_2 sites, and the oxygen environments of the Fe in the shorter chains is mostly tetrahedral. The unexpected behavior of the sample (a) could be reminiscent of the doped $K_2Cu_{1-x}Mn_xF_4$ (Ref. 23). The frozen iron spins in the chains are isoelectronic to the Mn^{2+} ions and their environment yields similar energy levels. Consequently, they could also impose an antiferromagnetic coupling with the neighboring Cu_2 spins. Further measurements are in progress to confirm this explanation.

CONCLUSION

We have studied the phase diagram of the iron doped compounds. The change at $x=0.03$ from a mixed phase to a collinear one can be well understood by the presence of very small moments on the Cu_1 sites. The nature of the collinear phase above $x=0.03$ (i.e., the sign of the Cu_1-Cu_2 exchange coupling) can be changed by an appropriate heat treatment, showing that it is controlled by the local iron environment. How exactly does this process happen? This is to be discussed through Mössbauer measurements.

ACKNOWLEDGMENTS

One of the authors (I.M.) would like to thank G. Uimin for stimulating discussions, and M. Hennion for a critical reading of the manuscript. She also thanks P. Molina for his technical assistance.

[1]T. J. Kistenmacher, W. A. Bryden, J. S. Morgan, K. Moorjani, Y. W. Du, Z. Q. Qiu, H. Tang, and J. C. Walker, Phys. Rev. B **36**, 8877 (1987).

[2]H. Alloul, P. Mendels, H. Casalta, J. F. Marucco, and J. Arabski, Physica C **185-189**, 1193 (1991).

[3]J. Rossat-Mignod, P. Burlet, M. J. Jurgens, C. Vettier, L. P. Regnault, J. Y. Henry, C. Ayache, L. Forro, H. Noel, M. Potel, P. Gougeon, and J. C. Levet, J. Phys. **49**, Suppl. No. 12, C8-2119 (1988); D. Petitgrand and G. Collin, Physica C **153**, 192 (1988).

[4]H. Kadowaki, M. Nishi, Y. Yamada, H. Takeya, H. Takei, S. M. Shapiro, and G. Shirane, Phys. Rev. B **37**, 7932 (1988).

[5]A. H. Moudden, G. Shirane, J. M. Tranquada, R. J. Birgenau, Y. Endoh, K. Yamada, Y. Hidaka, and T. Murakami, Phys. Rev. B **38**, 8720 (1988).

[6]J. W. Lynn, W. H. Li, H. A. Mook, B. C. Sales, and Z. Fisk, Phys. Rev. Lett. **60**, 2781 (1988).

[7]P. F. Miceli, J. M. Tarascon, L. H. Greene, P. Barboux, M. Giroud, D. A. Neumann, J. J. Rhyne, L. F. Schneemeyer, and J. Waszczak, Phys. Rev. B **38**, 2477 (1988); P. F. Miceli, J. M. Tarascon, P. Barboux, L. H. Greene, B. G. Bagley, G. W. Hull, M. Giroud, J. J. Rhyne, and D. A. Neumann, Phys. Rev. B **39**, 12 375 (1989).

[8]Y. Lu and B. R. Patton, J. Phys. Condens. Matter **2**, 9423 (1990).

[9]H. Claus, S. Yang, A. P. Paulikas, J. W. Downey, and B. W.

Veal, Physica C **171**, 205 (1990); R. J. Cava, B. Batlogg, C. H. Chen, E. A. Rietman, S. M. Zahurak, and D. Werder, Phys. Rev. B **36**, 5719 (1987).

[10]E. Suard, V. Caignaert, and I. Mirebeau (unpublished).

[11]I. Mirebeau, C. Bellouard, M. Hennion, G. Jehanno, V. Caignaert, A. J. Dianoux, T. E. Phillips, and K. Moorjani, Physica C **184**, 299 (1991).

[12]I. S. Lyubutin, V. G. Terziev, T. V. Dimitrieva, A. M. Balagurov, and S. Nasu, Physica C **195**, 383 (1992); I. S. Lyubutin, V. G. Terziev, S. V. Luchko, A. Ya. Shapiro, A. M. Balagurov, and G. A. Bonch-Osmolovskiy, Physica C **199**, 296 (1992); L. Bottyan, A. Janossy, A. Barcs, I. Furo, J. Dengler, and D. L. Nagy, Hyperfine Interactions **55**, 1228 (1990).

[13]J. L. Garcia-Munoz, J. Rodriguez-Carjaval, S. H. Kilcoyne, C. J. Boardman, and R. Cywinski, J. Magn. Magn. Mater. **104**, 555 (1992).

[14]I. Mirebeau, C. Bellouard, M. Hennion, V. Caignaert, and E. Suard, J. Appl. Phys. **73**, 5689 (1993).

[15]J. Rodriguez-Carvajal, Physica B **192**, 55 (1993).

[16]A. M. Balagurov, F. Bourée, I. S. Lyubutin, and I. Mirebeau, Physica C (to be published).

[17]G. Uimin and V. Stepanov, Ann. Phys. (Leipzig) **2**, 284 (1993); W. Selke and G. V. Uimin, Physica C **214**, 37 (1994); G. V. Uimin (unpublished).

[18]J. Rossat-Mignod, L. P. Regnault, C. Vettier, P. Burlet, J. Y. Henry, and G. Lapertot, Physica B **169**, 58 (1991); J. Rossat-Mignod, L. P. Regnault, P. Bourges, P. Burlet, C. Vettier, and J. Y. Henry, Physica B **192**, 109 (1993).

[19]D. I. Khomskii and K. I. Kugel, Solid State Commun. **13**, 763 (1963).

[20]A. Rykov, V. Caignaert, N. Nguyen, A. Maignan, E. Suard, and B. Raveau, Physica C **205**, 3 (1993).

[21]J. D. Jorgensen, B. W. Veal, A. P. Paulikas, L. J. Nowicki, G. W. Crabtree, H. Claus, and W. K. Kwok, Phys. Rev. B **41**, 1863 (1990).

[22]R. Sonntag, D. Holwein, T. Brückel, and G. Collin, Phys. Rev. Lett. **66**, 1497 (1991); V. Plakhty, A. Stratilatov, Yu. Cherenkov, V. Federov, S. K. Sinha, C. K. Loong, B. Gaulin, M. Vlasov, and S. Moshkin, Solid State Commun. **84**, 639 (1992).

[23]J. Ferré and M. Regis, Solid State Commun. **26**, 225 (1978).